Prophylaxis and Treatment of SARS-CoV-2 infection by an ACE2 Receptor Decoy

Takuya Tada[†], Belinda M. Dcosta[†], Hao Zhou and Nathaniel R. Landau[#]

Affiliation:

Department of Microbiology, NYU Grossman School of Medicine, New York, NY, USA.

[†] These authors have contributed equally to this work.

[#]Corresponding author:

Nathaniel R. Landau, Ph.D.

NYU Grossman School of Medicine

430 East 29th Street, Alexandria West Building, Rm 509, New York, NY 10016

Email: nathaniel.landau@med.nyu.edu

Phone: (212) 263-9197

Summary

The emergence of SARS-CoV-2 variants with highly mutated spike proteins has presented an obstacle to the use of monoclonal antibodies for the prevention and treatment of SARS-CoV-2 infection. We show that a high affinity receptor decoy protein in which a modified ACE2 ectodomain is fused to a single domain of an immunoglobulin heavy chain Fc region dramatically suppressed virus loads in mice upon challenge with a high dose of parental SARS-CoV-2 or Omicron variants. The decoy also potently suppressed virus replication when administered shortly post-infection. The decoy approach offers protection against the current viral variants and, potentially, against SARS-CoV-2 variants that may emerge with the continued evolution of the spike protein or novel viruses that use ACE2 for virus entry.

Introduction

Since the initial zoonosis of SARS-CoV-2 into humans, the virus has undergone rapid evolutionary adaptation to the new host with the appearance of variants with divergent spike proteins. The appearance of the earlier Variants of Concern (Alpha, Beta, Gamma and Delta), each with a few mutations in the receptor binding domain, were replaced by the sudden emergence of the highly divergent Omicron variant first reported in Botswana and South Africa (CDC, 2022). As the virus has continued to adapt to its human host, it has become increasingly transmissible as a result of mutations that increase the affinity of the spike protein for the ACE2 receptor. Omicron BA.1 rapidly became prevalent world-wide and then gave rise to the BA.2 subvariant (CDC, 2022) and more recently to the highly transmissible BA.2.12.1, BA.4, BA.5, BA.2.75 and XBB subvariants, some of which have increased affinity for ACE2 (Cao et al., 2022b; Yue et al., 2023).

The divergence of the spike protein has presented an obstacle both to the effectiveness of vaccines and to monoclonal antibody therapy. The Regeneron REGN-COV2 monoclonal antibody cocktail and Lilly monoclonal antibodies that had potent neutralizing activity against earlier Variants of Concern spikes (Baum et al., 2020; Chen et al., 2021a; Chen et al., 2021b; Hansel et al., 2010; Planas et al., 2021b; Tada et al., 2021a; Tada et al., 2022b; Tada et al., 2021b; Tada et al., 2022c; Wang et al., 2021; Weinreich et al., 2021; Weisblum et al., 2020) and had been highly effective at preventing hospitalization and morbidity of patients infected by the earlier Variants of Concern, were rendered ineffective by the heavily mutated spikes of the Omicron variants which escape neutralization (Cameroni et al., 2021; Cao et al., 2021; Hoffmann et al., 2021; Iketani et al., 2022; Liu et al., 2022; Planas et al., 2021a; Tada et al., 2022a; VanBlargan et al., 2022; Zhou et al., 2022). The Omicron variants pose an additional obstacle to the prophylactic use of monoclonal antibodies (Cameroni et al., 2021; Cao et al., 2021; Hoffmann et al., 2021; Iketani et al., 2022; Liu et al., 2022; Planas et al., 2021a; Tada et al., 2022a; VanBlargan et al., 2022; Zhou et al., 2022). The AstraZeneca dual monoclonal antibody cocktail Evusheld is

54 used primarily for prophylaxis in immunocompromised individuals for whom vaccination may be
55 ineffective (ClinicalTrials.gov,); however, both Evusheld antibodies have significantly decreased
56 neutralizing titers against the BA.1 and BA.2 variants which could affect the long-term
57 effectiveness of the therapy (Cao et al., 2021; Iketani et al., 2022; Liu et al., 2022; Planas et al.,
58 2021a; Tada et al., 2022a; Zhou et al., 2022). The Sotrovimab monoclonal antibody Vir-7831
59 retains activity against the earlier Variants of Concern but has substantially decreased neutralizing
60 titer against the BA.1 and BA.2 variants. Until recently, the only therapeutic monoclonal antibody
61 that neutralized the Omicron variants was LY-CoV1404 (Westendorf et al., 2022); however, recent
62 viral subvariants escape neutralization by the monoclonal antibody. In light of the continued
63 evolution of viral variants with mutated spike proteins, there is a need for improved treatment and
64 therapies that are less affected by spike protein variability.
65
66 The concept of decoy receptors for the treatment of virus infection was initially tried as a therapy
67 for HIV infection. Decoys are predicted to be less susceptible to escape by mutagenesis of the
68 viral spike protein and less like to induce an antibody response as they are derived from self-
69 protein sequences to which the immune system is tolerant. A soluble CD4 “immunoadhesin”, in
70 which the ectodomain of CD4 was fused to an immunoglobulin domain was previously reported
71 (Traunecker et al., 1989). Although the protein neutralized the virus by binding the gp120 subunit
72 of the viral envelope glycoprotein *in vitro* (Daar et al., 1990; Haim et al., 2009; Orloff et al., 1993;
73 Schenten et al., 1999; Sullivan et al., 1998), it failed to decrease virus loads when used to treat
74 patients. More recently the concept was revived using an adeno-associated virus vector
75 expressing an enhanced soluble eCD4-Ig decoy (Gardner et al., 2015; Spitsin et al., 2020).
76 Rhesus macaques treated with the vector were highly protected against a challenge with SHIV-
77 AD8 and SIVmac239 (Gardner et al., 2015; Spitsin et al., 2020).
78

79 We previously reported on a receptor decoy protein for SARS-CoV-2 termed a “microbody” in
80 which the ACE2 ectodomain is fused to the CH3 domain of an immunoglobulin IgG1 heavy chain
81 (Tada et al., 2020). Truncation of the Fc domain served to decrease the mass of the protein as
82 well as to prevent binding of the protein to cell surface Fcγ receptors (Maute et al., 2015). The
83 ACE2 ectodomain contained a point mutation (H345A) that inactivates the carboxypeptidase
84 activity of ACE2 (Guy et al., 2005) to prevent possible effects of the protein on blood pressure.
85 The protein potently neutralized the parental D614G virus and viruses with the variant of concern
86 spike proteins by binding to the viral spike protein, preventing association of the virus with cell
87 surface ACE2 (Tada et al., 2020). Because ACE2 binding is a conserved feature of all SARS-
88 CoV-2 spike proteins, the decoy is predicted to maintain its neutralizing activity against current,
89 as well as future virus variants, without being affected by mutations in the variant spike proteins.
90
91 In this report, we tested a decoy protein mutated to increase its affinity for the spike protein
92 containing a truncated Fc region for its ability to prevent and treat SARS-CoV-2 infection in mouse
93 models. We found that the recombinant protein was a potent prophylactic against both parental
94 SARS-CoV-2 and the Omicron variants and was an effective therapeutic that rapidly decreased
95 virus loads when administered post-infection. The findings confirm and extend findings from other
96 groups using decoy.Fc fusion proteins (Higuchi et al., 2021; Ikemura et al., 2022; Zhang et al.,
97 2022).

98 ## Results

99 **High affinity decoy inhibits SARS-CoV-2 infection and replication *in vitro*.**

100 We previously reported the construction of plasmid vectors expressing an ACE2 microbody
101 (pcACE2.mb) in which the ectodomain of human ACE2 is fused to the IgG1 CH3 domain and
102 soluble ACE2 (pcsACE2) that encodes the unfused ectodomain (Tada et al., 2020). To further
103 increase the potency of the microbody decoy protein, we induced the mutations
104 T27Y/L79T/N330Y reported by Chan *et al.* (Chan et al., 2020) that increase ACE2 affinity for the
105 SARS-CoV-2 spike protein (pcACE2.1mb) (**Figure 1A**). In addition, the proteins are mutated in
106 the catalytic active site at position 345 (H345A) to inactivate phosphohydrolase activity (Guy et
107 al., 2005), preventing possible effects on blood pressure, and contain a carboxy-terminal His-Tag
108 (**Figure 1A and 1B**). The decoy proteins were produced by transfection of ExpiCHO cells with
109 the expression vectors and then purified by affinity chromatography and size exclusion
110 chromatography (**Figure 1C**). The antiviral activity of the decoy proteins was tested in the
111 pseudotyped lentivirus neutralization assay. The results show that the ACE2.mb decoy
112 neutralized virus with the D614 spike protein with a potency 10-fold increase compared to sACE2
113 while the high affinity ACE2.1mb decoy increased neutralizing activity another 5-fold (**Figure 1D**).
114 The decoy neutralized virus with the D614G spike with a similar potency. The ACE2.1mb decoy
115 was also active against virus with the Alpha, Beta, Gamma and Delta spike proteins. Analysis of
116 decoy antiviral activity against live virus showed that the decoy suppressed the replication of USA-
117 WA1/2020 and the Omicron variants. The ACE2.1mb decoy was 35-fold and 4-fold more potent
118 than sACE2 and the ACE2.mb, respectively (**Figure 1E**). The decoys were active against BA.1
119 and BA.2 although the variants showed a degree of resistance with a 6.2-fold and 16-fold
120 decreased titer, respectively.

121

122 Avidity of the decoys for the spike protein was analyzed in two assays (Tada et al., 2020; Tada et
123 al., 2022b). The first was a virion binding assay that measured the binding of spike protein-

124 pseudotyped virions to bead-bound decoy protein. The results showed that the ACE2.1mb decoy
125 bound more avidly to virions than sACE2 or the ACE2.mb (**Supplementary Figure 1A**). The
126 second assay measured the binding of sACE2-nLuc, ACE2.mb-nLuc, ACE2.1mb-nLuc
127 decoy:nanoluciferase fusion proteins to bind to spike protein-expressing 293T cells
128 (**Supplementary Figure 1B and C**). The results confirmed the increased avidity of ACE2.1mb as
129 compared to sACE2 and ACE2.mb for spike protein binding and showed the increased potency
130 of the decoy for the Alpha, Beta, Gamma and Delta spikes and a 4- and 5.9-fold decrease in
131 binding to BA.1 and BA.2 spike proteins (**Supplementary Figure 1D**). Taken together, the results
132 showed that the ACE2.1mb decoy protein was a potent inhibitor of parental and variant SARS-
133 CoV-2.
134
135 **Increased half-life of microbody decoy *in vivo*.**
136 Fusion of Fc domains onto proteins has been used to increase their half-life *in vivo* (Czajkowsky
137 et al., 2012; Roopenian and Akilesh, 2007). To determine whether the truncated single IgG1 CH3
138 domain of the microbody decoy would extend its half-life and to determine the tissue localization
139 of the decoy, recombinant decoy proteins sACE2-nLuc and ACE2.1mb-nLuc were produced. The
140 fusion proteins were injected intraperitoneally (i.p.) and the mice were live-imaged over 3 days.
141 The results showed that the proteins localized mainly to the spleen and that the sACE2 decoy
142 was nearly undetectable after one day, the ACE2.1mb protein was detectable after 3 days (**Figure**
143 **2A**). To further analyze the tissue distribution of the ACE2.1mb-nLuc decoy and to understand
144 how the route of administration affects its distribution, The ACE2.1mb decoy was injected i.p. or
145 intravenously (i.v.) or instilled intranasally (i.n.) and 72 hrs post-administration, the amount of
146 decoy protein in different tissues was determined by measuring the luciferase activity in lysates
147 of individual organs. In mice injected i.p, the decoy localized mainly to the spleen, liver and serum
148 with a minor fraction in the lung. I.v. injection similarly localized the decoy to the spleen, liver and
149 serum but resulted in a 100-fold increase in localization to the lung. I.n. instillation resulted in

150 localization of the decoy to the lung and trachea, as might be expected, with a small amount of
151 the protein in the nasal tissues and serum (**Figure 2B**). To determine the half-life of the decoy *in*
152 *vivo*, the ACE2.1mb decoy was administered i.v. or i.n. and luciferase activity in the serum and
153 lung was measured over 20 days. The half-life of the i.v. injected or i.n. instilled decoy in the
154 serum was 5.2 and 5.1 days, respectively. In the lung, the half-life of the i.v. injected protein was
155 4.0 days and i.n. instilled protein was 7.6 days (**Figure 2C**). The increased half-life and localization
156 to the lung by the i.n. instilled protein suggests that this route of administration would be most
157 effective therapeutically while i.v. injection would also be effective.
158
159 **Decoy protects against SARS-CoV-2 infection.**
160 To test the ability of the high affinity decoy to prevent SARS-CoV-2 infection *in vivo*, hACE2KI
161 (Knockin) mice that have a knock-in of human ACE2 were administered 100 μg of ACE2.1mb
162 protein by i.p. or i.v. injection or i.n. instillation. One day later, the mice were challenged with a
163 high dose of SARS-CoV-2 USA-WA1/2020. For comparison, the mice were treated in parallel with
164 the REGN-CoV2 cocktail, a mixture of REGN10933 and REGN10987 that has been shown to
165 potently suppress SARS-CoV-2 replication in animal models (Baum et al., 2020). Viral RNA in the
166 lung was quantified 3 days post-infection (dpi), the day of at which virus loads peak (Bao et al.,
167 2020). The decoy strongly suppressed virus replication in the mice when administered either i.v.
168 or i.n. Injection of the decoy i.p decreased the virus load 108-fold compared to mock while i.v
169 injection decreased the virus load 15,700-fold and i.n. instillation decreased the virus load 26,500-
170 fold, a level at which the viral RNA could not be undetected (**Figure 3A and B**). The monoclonal
171 antibody cocktail closely mirrored the effect of the decoy protein in the three routes of
172 administration. To compare the effectiveness of the sACE2, ACE2.mb, ACE2.1mb decoys, the
173 proteins were injected i.v. and the mice were challenged with live virus. The results showed that
174 sACE2 was the least effective while the ACE2.1mb decoy caused the greatest decrease in virus
175 load (**Figure 3C**). Histological examination of the lung tissue of the mice showed a prominent

176 infiltration of immune cells in the untreated mice (**Figure 3D)** that was largely absent in mice
177 treated with sACE2 and completely prevented by treatment with the ACE2.1mb decoy. To
178 understand the kinetics with which the decoy protein suppressed virus replication, mice were
179 treated and then infected 24 hours later and viral RNA was measured every day over the course
180 of one week. The results showed the absence of detectable viral RNA in the lung over the time
181 course except for a small blip at 3-dpi; virus was not detected in the trachea over the time course
182 (**Figure 3E**). A dose-response analysis of the potency of the decoy administered i.v. and i.n.
183 showed that 100 μg of the protein suppressed virus replication to undetectable levels and that as
184 little as 10 μg suppressed virus replication 12-fold **(Supplementary Figure 2A)**; administration
185 i.n. was slightly more effective than i.v. at the 50 and 10 microgram doses. A dose-response
186 analysis of the REGN-COV2 cocktail showed that the potency of the decoy was similar to that of
187 the cocktail administered i.v or i.n. **(Supplementary Figure 2B).**
188
189 The efficacy of the decoy against the Omicron variants was tested in BALB/c mice which support
190 high levels of replication of the virus (Halfmann et al., 2022). As controls, the mice were treated
191 with the LY-CoV1404 monoclonal antibody which is active against the Omicron variant (Iketani et
192 al., 2022; Liu et al., 2022; Tada et al., 2022a) or with the REGN-COV2 cocktail which is inactive
193 against Omicron (Cameroni et al., 2021; Cao et al., 2021; Hoffmann et al., 2021; Iketani et al.,
194 2022; Liu et al., 2022; Planas et al., 2021a; Tada et al., 2022a; VanBlargan et al., 2022). The
195 following day, the mice were challenged with BA.1 or BA.2 virus. The decoy decreased the BA.1
196 virus load 56-fold by i.v. injection and BA.2,100-fold by i.n. instillation. The decreases were
197 comparable to that caused by LY-CoV1404 (**Figure 3F, left**). The REGN-COV2 cocktail had no
198 effect. The decoy was also active against BA.2. The decrease in virus load was not as dramatic
199 but was similar to that of the highly potent LY-CoV1404 at the same dose (**Figure 3F, right and**
200 **Supplementary Figure 2B)**. The durability of protection was analyzed by administering the decoy
201 at increasing times pre-infection. The results showed a high degree of protection when the decoy

202 was administered up to 2 days prior to infection and a moderate degree of protection 3-dpi (200-
203 fold decrease in virus load); the protection was lost 5-dpi (**Figure 3G)**.
204
205 **Decoy suppresses virus load post-infection.**
206 To determine whether the decoy could be used to treat an established infection, hACE2KI mice
207 were infected with USA-WA1/2020 and then treated 1-, 6-, 12- and 16-hours later injected i.p., i.v.
208 or instilled i.n. with the ACE2.1mb decoy or REGN-COV2 cocktail (**Figure 4A**). At 3-dpi, virus
209 loads in the lung were measured. I.p. injection of the decoy or monoclonal antibody had no effect
210 on virus load at any of the time points (**Figure 4B**). In contrast, 1-hour post-infection, the i.v.
211 injected decoy decreased the virus load 1,100-fold while i.n. instillation decreased the virus load
212 27,500-fold to an undetectable level. Virus loads were similarly decreased when the decoy was
213 administered 6 hours post-infection. At 12 hours post-infection, the i.v. injected decoy had no
214 significant effect while the i.n. instilled decoy decreased the virus load 20-fold, an effect that was
215 maintained at the 16-hour time point. The effect of the decoy was comparable to that of the REGN-
216 COV2 cocktail at all time points. The effect of the decoy was not as pronounced on Omicron BA.1
217 or BA.2 with decreases of 290-fold and 30-fold, respectively for the i.n. instilled decoy (**Figure**
218 **4C**). The effect of the decoy was 4-50-fold higher than LY-CoV1404 (**Figure 4C**).

219 **Discussion**

220 We report here that a high affinity ACE2 microbody decoy was highly effective both in the form of
221 a recombinant protein for the treatment of SARS-CoV-2 infection. The decoy was highly potent *in*
222 *vitro* against viruses with Variants of Concern spike proteins including Omicrons BA.1 and BA.2.
223 I.v. injection or i.n. instillation of the recombinant decoy protein prior to infection protected
224 hACE2KI mice from a high dose of live virus, suppressing virus replication to undetectable levels
225 and preventing lung pathology. The decoy was highly effective administered up to 3 days prior to
226 infection. Administration of the recombinant protein shortly after infection with SARS-CoV-2
227 rapidly suppressed virus replication in the lung. The decoy was at least as potent for prophylaxis
228 and treatment as potent emergency-use-authorized monoclonal antibodies. The addition of the
229 single CH3 IgG1 domain served to extend the half-life of the decoy and increased its avidity for
230 the spike protein while preventing absorbance of the protein to Fc receptors that would decrease
231 the concentration of the free protein.

232

233 This report confirms and extends recent findings from other groups using decoys containing full-
234 length Fc regions that were reported during the preparation of this manuscript. Hoshino's group
235 reported that an ACE2.Fc fusion protein containing mutations A25V, K31N and N90H
236 administered 2 hours post-infection increased the survival in the hamster model (Higuchi et al.,
237 2021; Ikemura et al., 2022). Zhang *et al.* reported that a high affinity receptor decoy termed
238 sACE2v2.4.Fc fusion protein containing mutations T27Y, L79T, and N330Y (Chan et al., 2020)
239 protected K18-ACE2 transgenic mice from infection with SARS-CoV-2 variants and protected
240 mice from disease when given 12- and 24-hours post-infection (Zhang et al., 2022).

241

242 I.v. injection or i.n. instillation of the decoy protein 1- or 6-hours after infection with USA-WA1/2020
243 decreased the virus load 10,000-fold, demonstrating the potency with which it suppresses virus
244 replication. Administration at later times (12- and 16-hours post-infection) was less effective,

245 decreasing virus loads by 100-fold. This timing should not be taken to mean that in humans decoy
246 therapy would need to be administered as soon post-infection. In the mouse model, virus
247 replication kinetics are somewhat faster than in humans, peaking 2-4-dpi, due to the high dose of
248 virus administered (Jones et al., 2021). In our study, the effect of the decoy was similar to that of
249 the therapeutic monoclonal antibodies which are effective at preventing hospitalization and death
250 when given during the symptomatic phase of infection, several dpi (Group et al., 2021; Razonable
251 et al., 2021). The decoy may act in humans with kinetics similar to that of anti-spike protein
252 monoclonal antibodies that neutralize virus by a similar mechanism. Results reported here with
253 the recombinant protein are consistent with those previously reported with a high affinity decoy
254 3N39v2 containing 4 mutations (Higuchi et al., 2021; Ikemura et al., 2022) and with the decoy
255 sACE2v2.4-Ig that showed protection against infection and disease in hamsters and transgenic
256 mouse models.
257
258 The antiviral effect of the decoy was influenced by its route of administration. I.p. injection
259 localized the protein mainly to the liver, serum and spleen. This route of decoy administration was
260 not effective as was the case for i.p. injected monoclonal antibody. I.v. injection resulted in a
261 higher concentration of the decoy in the lung and potent antiviral activity. I.n. instillation localized
262 the decoy primarily to the lung and trachea, as might be expected, and provided in the highest
263 degree of protection. The findings suggest that the decoy acts in the lung to suppress virus
264 replication and that both i.v and i.n. are effective routes of administration.
265
266 The decoy was less protective against the BA.1 and BA.2 subvariants both *in vitro* and *in vivo*
267 than against the parental USA-WA1/2020 virus. Its activity against the variants was comparable
268 to that of the potent therapeutic monoclonal antibody LY-CoV1404 suggesting that the decoy
269 would be similarly effective against these variants in clinical use. The decoy has increased

270 potency against the recent BA.2.75 (data not shown), suggesting that the virus is not mutating in
271 such a way as to decrease effectiveness of the decoy approach.
272
273 The rapid evolution of SARS-CoV-2 has presented an obstacle to the development of effective
274 therapies that target the spike protein. *In vitro* selection studies suggest that the spike protein will
275 continue to evolve over the next several years imposing further challenge to the development of
276 broadly neutralizing monoclonal antibodies (Schmidt et al., 2021). The receptor decoy approach
277 is more resistant to immuno-evasion by novel variants because of the requirement that the spike
278 protein preserves its affinity for ACE2. As new spike protein variants evolve, they are likely to
279 remain susceptible to neutralization by the decoy. As the virus has continued to evolve and
280 increase its transmissibility following zoonosis into humans, the variant spike proteins have
281 tended to increase their affinity for ACE2, resulting in increased sensitivity to neutralization by the
282 decoy (Cao et al., 2022a; Yue et al., 2023). It is conceivable that a variant will emerge that
283 switches its receptor usage to an alternative cell surface protein, thereby becoming resistant to
284 the decoy; however, such an event has not occurred in nature and extensive laboratory
285 mutagenesis of the spike protein has not resulted in a receptor switch (Greaney et al., 2021; Starr
286 et al., 2020). If such a switch were to occur in a pandemic coronavirus or virus of another virus
287 class, a receptor decoy could be developed based on its receptor and rapidly deployed.
288
289 **Limitations of Study**
290 The study is based on analyses of decoy receptor in hACE2KI mice. While these mice express
291 human ACE2 at physiological levels in the appropriate tissues, they may not entirely accurately
292 reflect the human. Calculations of how much protein would be required to treat humans may not
293 be accurate. Moreover, the time course of SARS-CoV-2 infection is longer in humans, and thus
294 the time courses analyzed here may not be directly translatable to human.
295

296 **Acknowledgements**

297 We thank Victor Torres and Juliana Ilmain (NYU Grossman School of Medicine) for assistance
298 with FPLC purification of recombinant proteins and Meike Dittman and Bruno Rodriguez-
299 Rodriguez for ACE2.TMPRSS2.Vero E6 cells. We thank members of the Experimental Pathology
300 Research Laboratory which is supported by NIH Grant P30CA016087 to the NYU Langone Laura
301 and Isaac Perlmutter Cancer Center for histology. The work was funded by grants from the NIH
302 to N.R.L. (DA046100, AI122390 and AI120898). T.T. was supported by the Vilcek/Goldfarb
303 Fellowship Endowment Fund.

304

305 **Author contributions**

306 T.T., B.M.D. and H.Z. conducted the experiments. T.T. designed the experiments and wrote the
307 paper. T.T. and B.M.D. did the statistical analysis. N.R.L. supervised the study and revised the
308 manuscript.

309

310 **Declaration of Interests**.

311 The authors declare no competing interests.

312 **Figure Legends**

313 **Figure 1. High affinity ACE2 decoy potently neutralizes SARS-CoV-2 variants.**

314 (A) The domain structure of soluble ACE2, ACE2mb and high affinity ACE2.1mb is shown. The
315 ectodomain is shaded green; transmembrane domain (TM), intracellular domain (IC), the IgG1
316 CH3 domain is indicated and carboxy-terminal 6XHis-tag are shown. The high affinity ACE2.1mb
317 decoy has mutations to increase spike protein affinity (T27Y, L79T, N330Y) and activate site point
318 mutation H345A to inactivate carboxypeptidase activity. The genes are cloned into expression
319 vector pcDNA3.1 in which transcription is driven by the cytomegalovirus promoter.

320 (B) The 3D structure of the ACE2 (green) and spike protein (purple) complex was generated
321 using PyMoL. The position of the mutations for improved decoy in the ACE2 carboxypeptidase
322 domain are shown.

323 (C) Recombinant decoy proteins produced in transfected ExpiCHO cells were purified by Ni-NTA
324 affinity chromatography followed by size-exclusion chromatography. Purity of the proteins (25μg)
325 were analyzed on a silver staining.

326 (D) Neutralizing activity of the decoy proteins was measured using the variant spike protein-
327 pseudotyped lentiviruses assay with a packaged luciferase expressing lentiviral genome.
328 Lentiviruses were pseudotyped by the ancestral spike, parental spike or Alpha, Beta, Gamma and
329 Delta spike protein. Vesicular stomatitis virus G protein (VSV-G) pseudotype served as a
330 specificity control. Variable amounts of decoy (indicated on the X-axis) were incubated with a
331 fixed amount of pseudotyped lentivirus (MOI=0.2). Infectivity (indicated on the Y-axis) is displayed
332 as the percent infection normalized to control untreated virus as determined by luciferase assay
333 of the infected cultures. The IC50s (nM) of decoy neutralization on each variant spike protein
334 pseudotyped virus is calculated using the neutralization curves is shown in the table below.

335 (E) 2-fold serial dilutions of decoy proteins were incubated with USA-WA1/2020, Omicron BA.1
336 or BA.2 virus (MOI=0.01) and added to Vero E6. After 2 days of infection, cells were harvested
337 and subgenomic E gene was quantified by RT-PCR. IC50s (nM) were calculated from curves

338 using Prism GraphPad 8 software and shown in the table. The experiment was done three times
339 with similar results.
340
341 **Figure 2. ACE2.1mb is stable *in vivo*.**
342 (A) C57BL/6 mice were injected i.p. with 100 μg of sACE2.nLuc or ACE2.1mb.nLuc
343 nanoluciferase fusion proteins. After 6, 12, 24, 48 and 72 hours of injection, the mice were imaged
344 with Nano-Glo substrate. The panel on the right shows a graph of the fluorescence in relative light
345 units (RLU).
346 (B) ACE2.1mb-nLuc (100 μg) was administered i.p., i.v. or i.n. to C57/BL6 mice (n=3). 3-dpi, nasal
347 epithelium, lung, trachea, spleen, thymus, liver and serum were harvested and luciferase activity
348 was quantified.
349 (C) ACE2.1mb-nLuc protein (100 μg) was administered by i.v. injection or i.n. installation. After
350 0.25, 1, 7, 10, 21 days, lungs and serum were harvested and luciferase activity was quantified.
351 The concentration and half-life of decoy was determined based on standard curve obtained from
352 the mixture of serial diluted ACE2.1mb-nLuc proteins and tissue lysate from wild-type (n=3). The
353 experiment was done twice with similar results.
354
355 **Figure 3. ACE2 decoy protects mice from SARS-CoV-2 infection and decreases virus loads.**
356 (A) Experimental scheme for decoy prophylaxis is shown. hACE2KI or BALB/c mice were injected
357 i.p., i.v. or i.n. with 100 μg of ACE2.1mb or REGN-COV2 or LY-CoV1404. One day post injection,
358 the mice were challenged with 2 X 10^4 PFU of SARS-CoV-2 USA-WA1/2020 (hACE2KI) or SARS-
359 CoV-2 Omicron BA.1 or BA.2 (BALB/c) and viral RNA copies were quantified 2-dpi (Omicron) or
360 3-dpi (WA1/2020).
361 (B) Viral RNA copies (WA1/2020) in lung were quantified 3-dpi.

362 (C) sACE2, ACE2.mb or ACE2.1mb proteins (100 μg) was administered to hACE2KI (n=5) by i.n.
363 instillation. The following day, the mice were challenged with 2 X 10^4 PFU of SARS-CoV-2 USA-
364 WA1/2020. 3 dpi, subgenomic viral E RNA in the lung was quantified by RT-qPCR.
365 (D) Hematoxylin and eosin (HE) staining of lung sections from SARS-CoV-2 WA1/2020 infected
366 mice. Mice were injected with sACE2, ACE2.1mb. Post 1 day of injection, mice were challenged
367 with SARS-CoV-2. 3-dpi, lung histology was visualized with HE staining. Scale bars, 200 μm (top),
368 50 μm (bottom).
369 (E) ACE2.1mb protein (100 μg) was administered to hACE2KI mice (n=4) by i.n. instillation and
370 the following day, challenged with 2 X 10^4 PFU of SARS-CoV-2 USA-WA1/2020. At 1-, 2-, 3-, 4-,
371 5-, 6- and 7-dpi, subgenomic viral E gene RNA in the lung and trachea were quantified. The
372 horizontal line indicates the level of detection determined using uninfected mouse tissues.
373 (F) BALB/c mice were injected i.v. or i.n. with 100 μg of ACE2.1mb or LY-CoV1404 antibody (n=4-
374 5). One day post injection, the mice were challenged with 2 X 10^4 PFU Omicron BA.1 (left) or
375 BA.2 (right). 2-dpi, lung subgenomic viral E RNA was quantified by RT-PCR. The copy numbers
376 detected in uninfected samples is the result of low-level background priming. Confidence intervals
377 are shown as the mean ± SD. **P ≤ 0.01, ***P≤0.001, ****P≤0.0001. The experiment was done
378 twice with similar results.
379 (G) hACE2KI mice were instilled i.n. with 100 μg of decoy proteins and then infected 0, 0.25, 1,
380 3, 5, and 7 days later with SARS-CoV-2 WA1/2020. At 3-dpi, lung subgenomic viral E RNA was
381 quantified by RT-qPCR.
382
383 **Figure 4. ACE2 decoy treats SARS-CoV-2 infection and decreases virus loads in mice.**
384 (A) Therapeutic experimental scheme for decoy treatment is shown. hACE2KI mice were infected
385 with USA-WA1/2020 virus (n=4-5) and BALB/c mice were infected with Omicron BA.1 or BA.2
386 virus via i.n. injection. After 1, 6, 12, 16 hours post infection, mice were treated with 100μg

387 ACE2.1mb or REGN-COV2 or LY-CoV1404 via i.p., i.v. or i.n. injection. Viral RNA copies in lung
388 were quantified 2-dpi (Omicron) or 3-dpi (WA1/2020). The copy numbers detected in uninfected
389 samples is the result of low-level background priming.
390 (B) After 1, 6, 12, 16 hours post infection, mice were treated with decoy. Viral RNA copies
391 (WA1/2020) in lung were quantified -dpi.
392 (C) After 6 hours post infection, mice were treated with decoy. Viral RNA copies (Omicron BA.1
393 (left) or BA.2 (right)) in lung were quantified 2-dpi. Confidence intervals are shown as the mean ±
394 SD. **P ≤ 0.01, ***P≤0.001, ****P≤0.0001. The experiment was done twice with similar results.

395 **STAR Methods**

396 **Resource Availability**

397 **Lead Contact**

398 Further information and requests for resources and reagents should be directed to and will be
399 fulfilled by the Lead Contact, Nathaniel R. Landau (nathaniel.landau@med.nyu.edu).

400

401 **Materials Availability**

402 All unique DNA constructs, proteins and pseudotyped virus generated in this study are available
403 from the Lead Contact upon request.

404

405 **Data and Code Availability**

406 • The data used in this study are available upon request from the lead contact.

407 • This paper does not report original code.

408 • Any additional information required to reanalyze the data reported in this paper is available
409 from the lead contact upon request.

410

411 **Experimental Model and Subject Details**

412 **Mice**

413 hACE2KI (B6.129S2(Cg)ACE2tm1(ACE2)Dwnt/J) and BALB/c mice were purchased from the
414 Jackson Laboratory. We collected as many mice as possible and used them for the experiments.
415 The sample size was described in the Figure legend. All animal experiments were done under
416 protocols approved by the NYU Langone Institutional Animal Care and Use Committee (#170304)
417 in accord with the standards set by the Animal Welfare Act. The study was approved by the NYU
418 School of Medicine Division of Comparative Medicine Standard Operating Protocol (40-008-17).
419 All experiments were done twice or triplicates with similar results.

420

421 **Cells**

422 293T and Vero E6 cells were cultured at 37°C under 5% CO_2 in Dulbecco's modified Eagle
423 medium (DMEM) supplemented with 10% fetal bovine serum (FBS) and penicillin/streptomycin.
424 ACE2.293T(Tada et al., 2020) and ACE2.TMPRSS2.Vero E6 cells were cultured with the addition
425 of puromycin (1 μg/ml). ExpiCHO-S cells (Thermo Fisher Scientific) were grown at 37 °C under
426 8% CO_2 in suspension in ExpiCHO serum-free expression medium in a shaking incubator.

427

428 **Plasmids**

429 The plasmids pLenti.GFP.nLuc, pMDL, pcRev, pcCOV2.S.delta19 and pcCOV2.S.delta19-variant
430 spikes used to produce spike protein-pseudotyped lentiviruses have been previously described
431 (Tada et al., 2020). The decoy expression vectors pcsACE2, pcACE2mb and pcACE2.H345A.mb
432 have been previously described (Tada et al., 2020). To construct the expression vector
433 pcACE2.1mb encoding the high affinity microbody decoy ACE2.1mb, point mutations T27Y, L79T,
434 N330Y were introduced into pcACE2.H345A.mb by overlap extension PCR and the amplicon was
435 cloned into the Kpn-I and Xho-I sites of pcDNA6. To construct the expression vector pcsACE2-
436 nLuc and pcsACE2.1mb-nLuc expressing a decoy:nanoluciferase protein, DNA fragments
437 encoding ACE2 amino acids 1-741 and nanoluciferase were amplified by PCR and joined by
438 overlap extension PCR using primers containing Kpn-I and Xho-I sites. The resulting amplicon
439 was cloned into Kpn-I and Xho-I cleaved pcDNA6. Nucleotide sequences of all plasmids were
440 confirmed by DNA sequencing.

441

442 **Monoclonal antibodies**

443 REGN-COV2 (REGN10933+REGN10987) were provided by Regeneron Pharmaceuticals.
444 Bebletovimab (LY-CoV1404) was obtained from discarded vials.

445

446 **Recombinant protein purification**

447 ExpiCHO-S cells (Thermo Fisher Scientific) cultured in shaker flasks in serum-free medium were
448 grown to a density of 6 X 10^6/ml and transfected with 400 μg of plasmid DNA using with 1.28 ml
449 of ExpiFectamine. After 12 hours, 2.4 ml of ExpiCHO Enhancer and 64 ml of ExpiCHO Feed were
450 added. After 4 days, the culture supernatant was collected and passed over a 0.22 μm filter. The
451 supernatant was passed over a 5 ml HiTrap Chelating column charged with nickel on an Akta
452 FPLC (GE healthcare). The column was washed with buffer containing 20 mM Tris pH 8, 150 mM
453 NaCl, 10mM imidazole and the bound protein was then eluted in buffer containing 250 mM
454 imidazole. The eluate was loaded onto a Superdex 200 size-exclusion column (GE healthcare) in
455 running buffer containing 10 mM Tris pH 7.4, 150 mM NaCl. Fractions were collected and those
456 containing peak protein concentrations were pooled. Protein purity was analyzed on a 4-12% Bis-
457 Tris SDS-PAGE by silver staining (Invitrogen).
458
459 **Method Details**
460
461 **Virion-decoy pull-down assay**
462 Decoy proteins (5, 2, 0.5 and 0.1 μg) were allowed to bind 30 μl of nickel-nitrilotriacetic acid-
463 agarose beads (QIAGEN) for 1 hour after which unbound decoy was removed by washing with
464 PBS. The beads were then incubated with 30 μl (30 μg) of D614G spike protein-pseudotyped
465 virus for 1 hour after which unbound virions were removed by washing with PBS. The bound
466 virions were then eluted from the beads with Laemmle loading buffer containing reducing agent
467 (Invitrogen) and analyzed on an immunoblot probed with anti-p24 monoclinal antibody AG3.0
468 (Creative Biolabs) and horseradish peroxidase (HRP)-conjugated goat anti-mouse IgG secondary
469 antibody (Sigma-Aldrich). The signals were developed with Luminata Crescendo Western HRP
470 Substrate (Millipore) and membranes were visualized on an iBright imaging system (Invitrogen)
471 (Tada et al., 2020).

472

473 **Cell-based decoy spike binding assay**

474 293T cells (2 x 10^6) were transfected with 2 μg spike expression vector by lipofection using
475 lipofectamine 2000 (Invitrogen). One day post-transfection, the cells were plated in a 96 well plate
476 at 1 X 10^4 cells/well. The following day, decoy-nLuc fusion protein was added to the wells. After
477 30 minutes, the free fusion protein was removed by washing with PBS and cell-bound luciferase
478 activity was measured using NanoGlo luciferase substrate (Nanolight) in an Envision 2103
479 microplate luminometer (PerkinElmer) (Tada et al., 2022b).

480

481 **Pseudotyped lentiviral neutralization assay**

482 Spike protein-pseudotyped lentiviruses were generated as previously described (Tada et al.,
483 2020). Briefly, virus stocks were generated by cotransfection of 293T cells with pMDL,
484 pLenti.GFP.nLuc, pcCoV2.S-Δ19 and pRSV.Rev using the calcium phosphate method. After 2
485 days, the culture supernatant was harvested and the virus was concentrated by ultracentrifugation
486 at 4°C for 1 hour at 30,000 X g and normalized for reverse transcriptase (RT) activity. To
487 determine the neutralizing titer of the decoy proteins, serially diluted decoys were incubated with
488 pseudotyped virus (MOI=0.2) for 30 minutes at room temperature and then added to ACE2.293T
489 or ACE2.TMPRSS2.Vero E6 cells. At 2-dpi, luminescence was measured in an Envision 2103
490 microplate luminometer (PerkinElmer). All samples were assayed in duplicate and IC50s were
491 calculate by Prism 8 software.

492

493 **Decoy localization *in vivo***

494 100 μg of ACE2.1mb-nLuc or sACE2-nLuc proteins were injected intraperitoneal (i.p.),
495 intravenous (i.v.) or by intranasal (i.n.) instillation. After 6, 12, 24, 48, 72 hours, the mice were
496 sacrificed and the tissues were homogenized in lysing matrix D tubes (MP Biomedicals) with a

497 FastPrep-24 5G homogenizer (MP Biomedicals). Blood was collected by submandibular bleeding
498 and serum was harvested. The tissue lysates were mixed with an equal volume of Nano-GLO
499 Luciferase Assay Reagent (Nanolight) and luciferase activity was quantified on an Envision 2103
500 plate reader (PerkinElmer). Decoy concentration and half-life were determined based on a
501 standard curve derived from the mixture of serial diluted ACE2.1mb-nLuc proteins and tissue
502 lysate from wild-type. For live imaging of the decoy, mice were injected i.p. with 100 µl 1:40 diluted
503 Nano-GLO substrate. After 3 minutes, the mice were live imaged on an IVIS Lumina III XR
504 (PerkinElmer).
505
506 **Preparation of live virus**
507 SARS-CoV-2 WA1/2020 P1 virus stock (BEI Resources, NR-52281) was amplified by a second
508 round of replication on Vero E6 cells infected at MOI=0.01. At 3-dpi, the culture medium was
509 harvested, filtered through a 0.45 μm filter and frozen at -80°C in aliquots. The virus was titered
510 by plaque assay on Vero E6 cells (Wei et al., 2020). SARS-CoV-2 Omicron BA.1 (BEI Resources,
511 NR56461) and BA.2 stocks (BEI Resources, NR-56781) were grown on ACE2.TMPRSS2.Vero
512 E6 cells infected at an MOI=0.1. The P1 stock was amplified by a second round of replication on
513 ACE2.TMPRSS2.Vero E6 cells infected at MOI=0.01. The virus-containing supernatant was
514 filtered through a 0.45 μm filter, concentrated by passage through an Amicon filter (Millipore) and
515 stored in aliquots at -80°C. The virus was titered by plaque assay on Vero E6 cells. Live virus was
516 handled by trained personnel in a Biosafety level 3 facility.
517
518 **Prophylaxis and treatment of mice with decoy proteins**
519 For prophylaxis, 6-8 weeks old hACE2KI or BALB/c mice were anesthetized with isoflurane and
520 injected i.v. with decoy or monoclonal antibody, or alternatively, were anesthetized with ketamine–
521 xylazine cocktail and administered the proteins by i.n. instillation. After 1 day, the mice were
522 infected i.n. with 2 X 10^4 PFU USA-WA1/2020 (hACE2KI) or Omicron BA.1 or Omicron BA.2

523 (BALB/c). At 2-dpi for Omicron-infected mice or 3-dpi for USA-WA1/2020-infected mice, the mice
524 were sacrificed and lungs and trachea were harvested and homogenized. Littermate controls
525 were included in all experiments. RNA was prepared from 200 µl of the lysate using the Quick-
526 RNA MiniPrep kit (Zymo Research). For treatment experiments, hACE2KI mice were infected with
527 2 X 10^4 PFU of SARS-CoV-2 USA-WA1/2020 i.n. At 1-, 6-, 12- or 16-hours post-infection, mice
528 were administered therapeutic monoclonal antibodies or decoy protein (100 µg) i.p., i.v. or i.n. 3-
529 dpi, lung and trachea were harvested and SARS-CoV-2 subgenomic E gene levels were
530 quantified by RT-qPCR.
531
532 **RT-qPCR**
533 Virus loads were measured by quantification of subgenomic viral E gene by RT-qPCR with
534 TaqMan probes. Cellular RNA was mixed with TaqMan Fast Virus 1-step Master Mix (Applied
535 Biosystems), 10 mM forward and reverse primers and 2 mM probe. PCR cycles were 95°C for
536 20s, 95°C for 3s, 40 cycles at 60°C for 30s) using forward primer E Sarbeco F
537 (ACAGGTACGTTAATAGTTAATAGCGT), reverse primer E Sarbeco R
538 (ATATTGCAGCAGTACGCACACA) and probe E Sarbeco P1(FAM-
539 ACACTAGCCATCCTTACTGCGCTTCG-BHQ1) (Corman et al., 2020). E gene subgenomic RNA
540 copies were measured using forward primer subgenomic F (CGATCTCTTGTAGATCTGTTCTC)
541 (Emma S. Winkler, 2022), reverse primer E Sarbeco R and probe E Sarbeco P1). Absolute copy
542 numbers were determined by normalization to a standard curve generated with *in vitro* transcribed
543 synthetic RNA containing the E gene sequence (2019-nCoV_E Positive Control, IDT: 10006896).
544 Cell lysate GAPDH copy numbers were measured as a control using mGAPDH.forward
545 (CAATGTGTCCGTCGTGGATCT) and mGAPDH.reverse (GTCCTCAGTGTAGCCCAAGATG)
546 with mGAPDH probe (CGTGCCGCCTGGAGAAACCTGCC). Data from tissue analyses was
547 normalized to GAPDH. Virus load was determined by the 2−ΔΔCTmethod).
548

549 **Histology**

550 Mice were infected with USA-WA1/2020 and sacrificed 3-dpi. Tissues were fixed in 10% buffered
551 formalin and processed through graded ethanol and xylene solutions and then embedded in
552 paraffin with a Leica Peloris automated processor. Five-micron sections were deparaffinized and
553 stained with hematoxylin and eosin on a Leica ST5020 automated histochemical stainer. The
554 slides were scanned at 40X on a Leica AT2 whole slide scanner.

555

556 **Data analysis and statistics**

557 All experiments were in technical duplicates or triplicates. Statistical significance was determined
558 by the two-tailed, unpaired t test using GraphPad Prism (Version 8) software. Significance was
559 based on two-sided testing. Confidence intervals are shown as the mean ± SD. (*P≤ 0.05, **P≤
560 0.01, ***P≤0.001, ****P≤0.0001).

561 **References**

562 Bao, L., Deng, W., Huang, B., Gao, H., Liu, J., Ren, L., Wei, Q., Yu, P., Xu, Y., Qi, F.*, et al.*
563 (2020). The pathogenicity of SARS-CoV-2 in hACE2 transgenic mice. Nature *583*, 830-833.
564 Baum, A., Ajithdoss, D., Copin, R., Zhou, A., Lanza, K., Negron, N., Ni, M., Wei, Y.,
565 Mohammadi, K., Musser, B.*, et al.* (2020). REGN-COV2 antibodies prevent and treat SARS-
566 CoV-2 infection in rhesus macaques and hamsters. Science *370*, 1110-1115.
567 Cameroni, E., Bowen, J.E., Rosen, L.E., Saliba, C., Zepeda, S.K., Culap, K., Pinto, D.,
568 VanBlargan, L.A., De Marco, A., di Iulio, J.*, et al.* (2021). Broadly neutralizing antibodies
569 overcome SARS-CoV-2 Omicron antigenic shift. Nature.
570 Cao, Y., Wang, J., Jian, F., Xiao, T., Song, W., Yisimayi, A., Huang, W., Li, Q., Wang, P., An,
571 R.*, et al.* (2021). Omicron escapes the majority of existing SARS-CoV-2 neutralizing antibodies.
572 Nature.
573 Cao, Y., Yisimayi, A., Jian, F., Song, W., Xiao, T., Wang, L., Du, S., Wang, J., Li, Q., Chen, X.*,*
574 *et al.* (2022a). BA.2.12.1, BA.4 and BA.5 escape antibodies elicited by Omicron infection.
575 Nature *608*, 593-602.
576 Cao, Y., Yisimayi, A., Jian, F., Song, W., Xiao, T., Wang, L., Du, S., Wang, J., Li, Q., Chen, X.*,*
577 *et al.* (2022b). BA.2.12.1, BA.4 and BA.5 escape antibodies elicited by Omicron infection.
578 Nature.
579 CDC (2022). Omicron Variant: What You Need to Know.
580 Chan, K.K., Dorosky, D., Sharma, P., Abbasi, S.A., Dye, J.M., Kranz, D.M., Herbert, A.S., and
581 Procko, E. (2020). Engineering human ACE2 to optimize binding to the spike protein of SARS
582 coronavirus 2. Science *369*, 1261-1265.
583 Chen, R.E., Winkler, E.S., Case, J.B., Aziati, I.D., Bricker, T.L., Joshi, A., Darling, T.L., Ying, B.,
584 Errico, J.M., Shrihari, S.*, et al.* (2021a). In vivo monoclonal antibody efficacy against SARS-
585 CoV-2 variant strains. Nature *596*, 103-108.

586 Chen, R.E., Zhang, X., Case, J.B., Winkler, E.S., Liu, Y., VanBlargan, L.A., Liu, J., Errico, J.M.,
587 Xie, X., Suryadevara, N.*, et al.* (2021b). Resistance of SARS-CoV-2 variants to neutralization by
588 monoclonal and serum-derived polyclonal antibodies. Nat Med.
589 ClinicalTrials.gov phase III Double-blind, Placebo-controlled Study of AZD7442 for Pre-
590 exposure Prophylaxis of COVID-19 in Adult. (PROVENT).
591 Czajkowsky, D.M., Hu, J., Shao, Z., and Pleass, R.J. (2012). Fc-fusion proteins: new
592 developments and future perspectives. EMBO Mol Med *4*, 1015-1028.
593 Daar, E.S., Li, X.L., Moudgil, T., and Ho, D.D. (1990). High concentrations of recombinant
594 soluble CD4 are required to neutralize primary human immunodeficiency virus type 1 isolates.
595 Proc Natl Acad Sci U S A *87*, 6574-6578.
596 Gardner, M.R., Kattenhorn, L.M., Kondur, H.R., von Schaewen, M., Dorfman, T., Chiang, J.J.,
597 Haworth, K.G., Decker, J.M., Alpert, M.D., Bailey, C.C.*, et al.* (2015). AAV-expressed eCD4-Ig
598 provides durable protection from multiple SHIV challenges. Nature *519*, 87-91.
599 Greaney, A.J., Starr, T.N., Gilchuk, P., Zost, S.J., Binshtein, E., Loes, A.N., Hilton, S.K.,
600 Huddleston, J., Eguia, R., Crawford, K.H.D.*, et al.* (2021). Complete Mapping of Mutations to the
601 SARS-CoV-2 Spike Receptor-Binding Domain that Escape Antibody Recognition. Cell Host
602 Microbe *29*, 44-57 e49.
603 Group, A.-T.L.-C.S., Lundgren, J.D., Grund, B., Barkauskas, C.E., Holland, T.L., Gottlieb, R.L.,
604 Sandkovsky, U., Brown, S.M., Knowlton, K.U., Self, W.H.*, et al.* (2021). A Neutralizing
605 Monoclonal Antibody for Hospitalized Patients with Covid-19. N Engl J Med *384*, 905-914.
606 Guy, J.L., Jackson, R.M., Jensen, H.A., Hooper, N.M., and Turner, A.J. (2005). Identification of
607 critical active-site residues in angiotensin-converting enzyme-2 (ACE2) by site-directed
608 mutagenesis. FEBS J *272*, 3512-3520.
609 Haim, H., Si, Z., Madani, N., Wang, L., Courter, J.R., Princiotto, A., Kassa, A., DeGrace, M.,
610 McGee-Estrada, K., Mefford, M.*, et al.* (2009). Soluble CD4 and CD4-mimetic compounds inhibit
611 HIV-1 infection by induction of a short-lived activated state. PLoS Pathog *5*, e1000360.

612 Halfmann, P.J., Iida, S., Iwatsuki-Horimoto, K., Maemura, T., Kiso, M., Scheaffer, S.M., Darling,
613 T.L., Joshi, A., Loeber, S., Singh, G.*, et al.* (2022). SARS-CoV-2 Omicron virus causes
614 attenuated disease in mice and hamsters. Nature *603*, 687-692.
615 Hansel, T.T., Kropshofer, H., Singer, T., Mitchell, J.A., and George, A.J. (2010). The safety and
616 side effects of monoclonal antibodies. Nat Rev Drug Discov *9*, 325-338.
617 Higuchi, Y., Suzuki, T., Arimori, T., Ikemura, N., Mihara, E., Kirita, Y., Ohgitani, E., Mazda, O.,
618 Motooka, D., Nakamura, S.*, et al.* (2021). Engineered ACE2 receptor therapy overcomes
619 mutational escape of SARS-CoV-2. Nature Communications *12*, 3802.
620 Hoffmann, M., Krüger, N., Schulz, S., Cossmann, A., Rocha, C., Kempf, A., Nehlmeier, I.,
621 Graichen, L., Moldenhauer, A.-S., Winkler, M.S.*, et al.* (2021). The Omicron variant is highly
622 resistant against antibody-mediated neutralization: Implications for control of the COVID-19
623 pandemic. Cell.
624 Ikemura, N., Taminishi, S., Inaba, T., Arimori, T., Motooka, D., Katoh, K., Kirita, Y., Higuchi, Y.,
625 Li, S., Suzuki, T.*, et al.* (2022). An engineered ACE2 decoy neutralizes the SARS-CoV-2
626 Omicron variant and confers protection against infection in vivo. Sci Transl Med *14*, eabn7737.
627 Iketani, S., Liu, L., Guo, Y., Liu, L., Chan, J.F.W., Huang, Y., Wang, M., Luo, Y., Yu, J., Chu, H.*,*
628 *et al.* (2022). Antibody evasion properties of SARS-CoV-2 Omicron sublineages. Nature *604*,
629 553-556.
630 Jones, T.C., Biele, G., Muhlemann, B., Veith, T., Schneider, J., Beheim-Schwarzbach, J.,
631 Bleicker, T., Tesch, J., Schmidt, M.L., Sander, L.E.*, et al.* (2021). Estimating infectiousness
632 throughout SARS-CoV-2 infection course. Science *373*.
633 Liu, L., Iketani, S., Guo, Y., Chan, J.F.W., Wang, M., Liu, L., Luo, Y., Chu, H., Huang, Y., Nair,
634 M.S.*, et al.* (2022). Striking antibody evasion manifested by the Omicron variant of SARS-CoV-
635 2. Nature *602*, 676-681.
636 Maute, R.L., Gordon, S.R., Mayer, A.T., McCracken, M.N., Natarajan, A., Ring, N.G., Kimura,
637 R., Tsai, J.M., Manglik, A., Kruse, A.C.*, et al.* (2015). Engineering high-affinity PD-1 variants for

638 optimized immunotherapy and immuno-PET imaging. Proc Natl Acad Sci U S A *112*, E6506-
639 6514.
640 Orloff, S.L., Kennedy, M.S., Belperron, A.A., Maddon, P.J., and McDougal, J.S. (1993). Two
641 mechanisms of soluble CD4 (sCD4)-mediated inhibition of human immunodeficiency virus type
642 1 (HIV-1) infectivity and their relation to primary HIV-1 isolates with reduced sensitivity to sCD4.
643 J Virol *67*, 1461-1471.
644 Planas, D., Saunders, N., Maes, P., Guivel-Benhassine, F., Planchais, C., Buchrieser, J.,
645 Bolland, W.-H., Porrot, F., Staropoli, I., Lemoine, F.*, et al.* (2021a). Considerable escape of
646 SARS-CoV-2 Omicron to antibody neutralization. Nature.
647 Planas, D., Veyer, D., Baidaliuk, A., Staropoli, I., Guivel-Benhassine, F., Rajah, M.M.,
648 Planchais, C., Porrot, F., Robillard, N., Puech, J.*, et al.* (2021b). Reduced sensitivity of SARS-
649 CoV-2 variant Delta to antibody neutralization. Nature *596*, 276-280.
650 Razonable, R.R., Pawlowski, C., O'Horo, J.C., Arndt, L.L., Arndt, R., Bierle, D.M., Borgen, M.D.,
651 Hanson, S.N., Hedin, M.C., Lenehan, P.*, et al.* (2021). Casirivimab-Imdevimab treatment is
652 associated with reduced rates of hospitalization among high-risk patients with mild to moderate
653 coronavirus disease-19. EClinicalMedicine *40*, 101102.
654 Roopenian, D.C., and Akilesh, S. (2007). FcRn: the neonatal Fc receptor comes of age. Nat
655 Rev Immunol *7*, 715-725.
656 Schenten, D., Marcon, L., Karlsson, G.B., Parolin, C., Kodama, T., Gerard, N., and Sodroski, J.
657 (1999). Effects of soluble CD4 on simian immunodeficiency virus infection of CD4-positive and
658 CD4-negative cells. J Virol *73*, 5373-5380.
659 Schmidt, F., Weisblum, Y., Rutkowska, M., Poston, D., DaSilva, J., Zhang, F., Bednarski, E.,
660 Cho, A., Schaefer-Babajew, D.J., Gaebler, C.*, et al.* (2021). High genetic barrier to SARS-CoV-2
661 polyclonal neutralizing antibody escape. Nature *600*, 512-516.
662 Spitsin, S., Schnepp, B.C., Connell, M.J., Liu, T., Dang, C.M., Pappa, V., Tustin, R., Kinder, A.,
663 Johnson, P.R., and Douglas, S.D. (2020). Protection against SIV in Rhesus Macaques Using

664 Albumin and CD4-Based Vector-Mediated Gene Transfer. Molecular therapy Methods & clinical
665 development *17*, 1088-1096.
666 Starr, T.N., Greaney, A.J., Hilton, S.K., Ellis, D., Crawford, K.H.D., Dingens, A.S., Navarro, M.J.,
667 Bowen, J.E., Tortorici, M.A., Walls, A.C.*, et al.* (2020). Deep Mutational Scanning of SARS-CoV-
668 2 Receptor Binding Domain Reveals Constraints on Folding and ACE2 Binding. Cell *182*, 1295-
669 1310 e1220.
670 Sullivan, N., Sun, Y., Binley, J., Lee, J., Barbas, C.F., 3rd, Parren, P.W., Burton, D.R., and
671 Sodroski, J. (1998). Determinants of human immunodeficiency virus type 1 envelope
672 glycoprotein activation by soluble CD4 and monoclonal antibodies. J Virol *72*, 6332-6338.
673 Tada, T., Dcosta, B.M., Samanovic, M.I., Herati, R.S., Cornelius, A., Zhou, H., Vaill, A.,
674 Kazmierski, W., Mulligan, M.J., and Landau, N.R. (2021a). Convalescent-Phase Sera and
675 Vaccine-Elicited Antibodies Largely Maintain Neutralizing Titer against Global SARS-CoV-2
676 Variant Spikes. mBio *12*, e0069621.
677 Tada, T., Fan, C., Chen, J.S., Kaur, R., Stapleford, K.A., Gristick, H., Dcosta, B.M., Wilen, C.B.,
678 Nimigean, C.M., and Landau, N.R. (2020). An ACE2 Microbody Containing a Single
679 Immunoglobulin Fc Domain Is a Potent Inhibitor of SARS-CoV-2. Cell Rep *33*, 108528.
680 Tada, T., Zhou, H., Dcosta, B.M., Samanovic, M.I., Chivukula, V., Herati, R.S., Hubbard, S.R.,
681 Mulligan, M.J., and Landau, N.R. (2022a). Increased resistance of SARS-CoV-2 Omicron
682 variant to neutralization by vaccine-elicited and therapeutic antibodies. EBioMedicine *78*,
683 103944.
684 Tada, T., Zhou, H., Dcosta, B.M., Samanovic, M.I., Cornelius, A., Herati, R.S., Mulligan, M.J.,
685 and Landau, N.R. (2022b). High-titer neutralization of Mu and C.1.2 SARS-CoV-2 variants by
686 vaccine-elicited antibodies of previously infected individuals. Cell Rep *38*, 110237.
687 Tada, T., Zhou, H., Dcosta, B.M., Samanovic, M.I., Mulligan, M.J., and Landau, N.R. (2021b).
688 Partial resistance of SARS-CoV-2 Delta variants to vaccine-elicited antibodies and convalescent
689 sera. iScience *24*, 103341.

690 Tada, T., Zhou, H., Samanovic, M.I., Dcosta, B.M., Cornelius, A., Herati, R.S., Mulligan, M.J.,
691 and Landau, N.R. (2022c). Neutralization of SARS-CoV-2 Variants by mRNA and Adenoviral
692 Vector Vaccine-Elicited Antibodies. Front Immunol *13*, 797589.
693 Traunecker, A., Schneider, J., Kiefer, H., and Karjalainen, K. (1989). Highly efficient
694 neutralization of HIV with recombinant CD4-immunoglobulin molecules. Nature *339*, 68-70.
695 VanBlargan, L.A., Errico, J.M., Halfmann, P.J., Zost, S.J., Crowe, J.E., Jr., Purcell, L.A.,
696 Kawaoka, Y., Corti, D., Fremont, D.H., and Diamond, M.S. (2022). An infectious SARS-CoV-2
697 B.1.1.529 Omicron virus escapes neutralization by therapeutic monoclonal antibodies. Nat Med.
698 Wang, P., Nair, M.S., Liu, L., Iketani, S., Luo, Y., Guo, Y., Wang, M., Yu, J., Zhang, B., Kwong,
699 P.D.*, et al.* (2021). Antibody resistance of SARS-CoV-2 variants B.1.351 and B.1.1.7. Nature
700 *593*, 130-135.
701 Weinreich, D.M., Sivapalasingam, S., Norton, T., Ali, S., Gao, H., Bhore, R., Musser, B.J., Soo,
702 Y., Rofail, D., Im, J.*, et al.* (2021). REGN-COV2, a Neutralizing Antibody Cocktail, in Outpatients
703 with Covid-19. N Engl J Med *384*, 238-251.
704 Weisblum, Y., Schmidt, F., Zhang, F., DaSilva, J., Poston, D., Lorenzi, J.C.C., Muecksch, F.,
705 Rutkowska, M., Hoffmann, H.-H., Michailidis, E.*, et al.* (2020). Escape from neutralizing
706 antibodies by SARS-CoV-2 spike protein variants. eLife *9*, e61312.
707 Westendorf, K., Zentelis, S., Wang, L., Foster, D., Vaillancourt, P., Wiggin, M., Lovett, E., van
708 der Lee, R., Hendle, J., Pustilnik, A.*, et al.* (2022). LY-CoV1404 (bebtelovimab) potently
709 neutralizes SARS-CoV-2 variants. Cell Rep *39*, 110812.
710 Yue, C., Song, W., Wang, L., Jian, F., Chen, X., Gao, F., Shen, Z., Wang, Y., Wang, X., and
711 Cao, Y. (2023). Enhanced transmissibility of XBB.1.5 is contributed by both strong ACE2
712 binding and antibody evasion. bioRxiv, 2023.2001.2003.522427.
713 Zhang, L., Narayanan, K.K., Cooper, L., Chan, K.K., Skeeters, S.S., Devlin, C.A., Aguhob, A.,
714 Shirley, K., Rong, L., Rehman, J.*, et al.* (2022). An ACE2 decoy can be administered by

715 inhalation and potently targets omicron variants of SARS-CoV-2. EMBO Molecular Medicine *14*,
716 e16109.
717 Zhou, H., Dcosta, B.M., Landau, N.R., and Tada, T. (2022). Resistance of SARS-CoV-2
718 Omicron BA.1 and BA.2 Variants to Vaccine-Elicited Sera and Therapeutic Monoclonal
719 Antibodies. Viruses *14*.
720

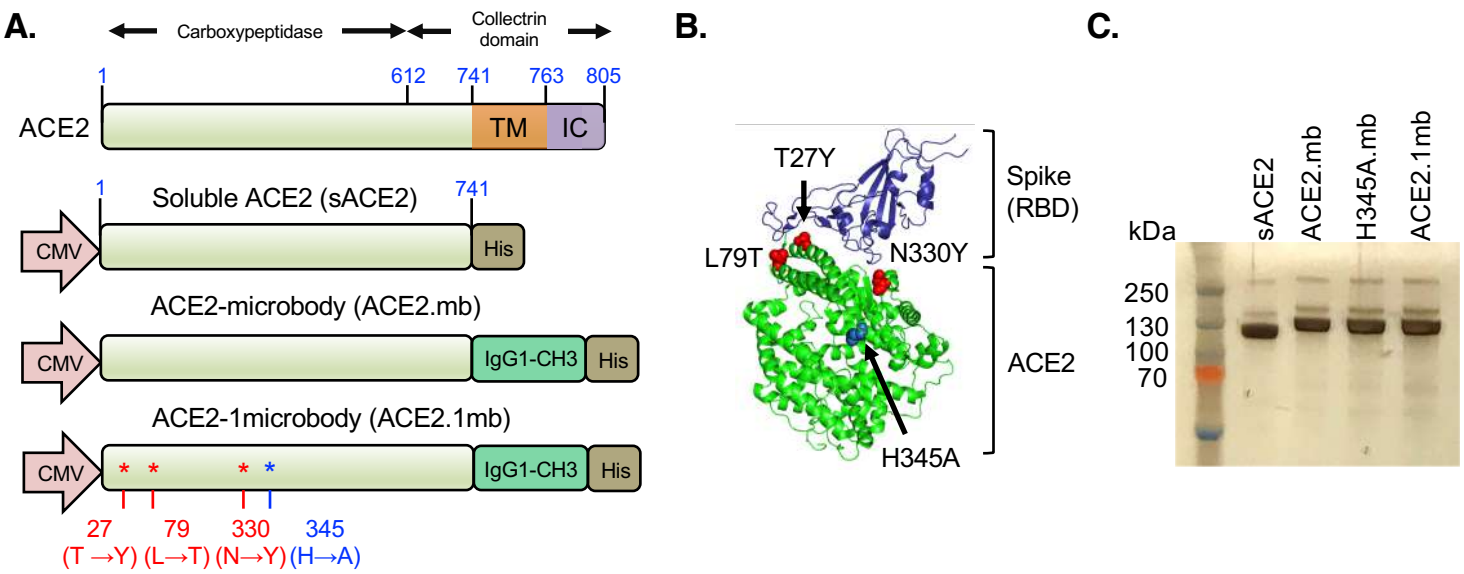

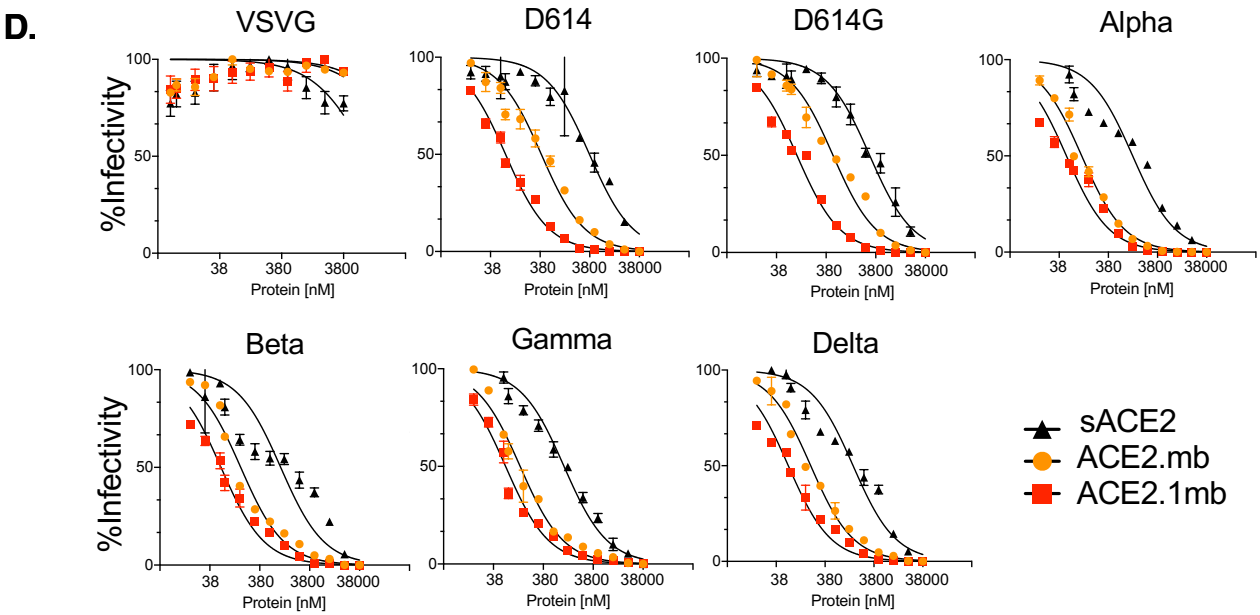

	IC50 (nM)						
	VSVG	D614	D614G	Alpha	Beta	Gamma	Delta
sACE2	ND	3,753	3,173	1,186	1,010	988	3,616
ACE2.mb	ND	402	523	109	158	130	391
ACE2.1mb	ND	76	98	54	65	67	100

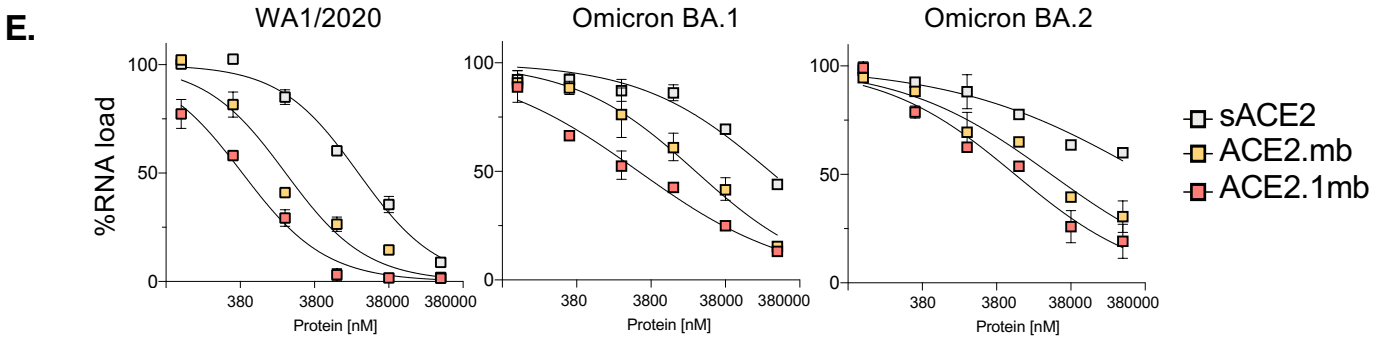

	IC50 (nM)		
	WA1/2020	Omicron BA.1	Omicron BA.2
sACE2	14,820	151,240	403,560
ACE2.mb	1,558	15,124	20,596
ACE2.1mb	418	2,584	6,726

Figure. 1

A.

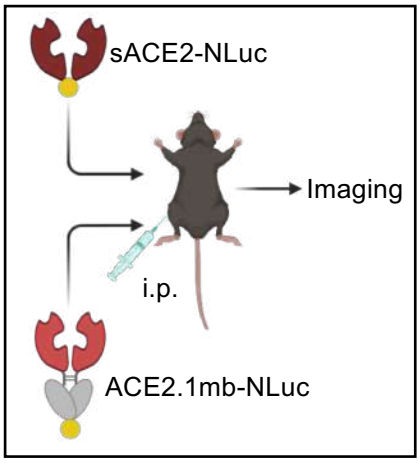

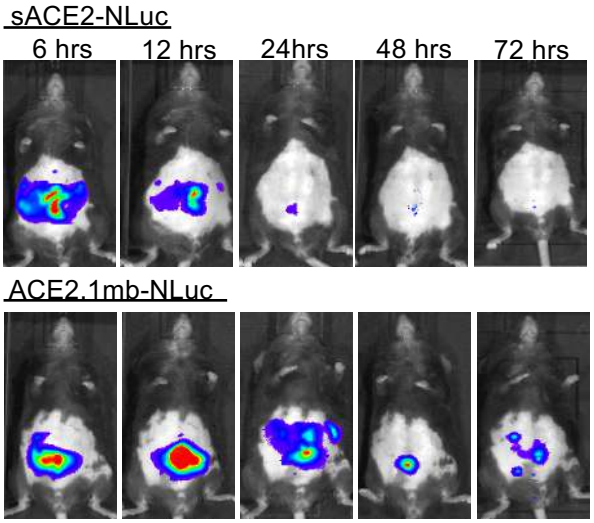

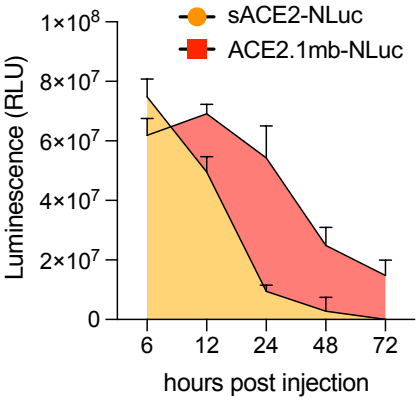

B.

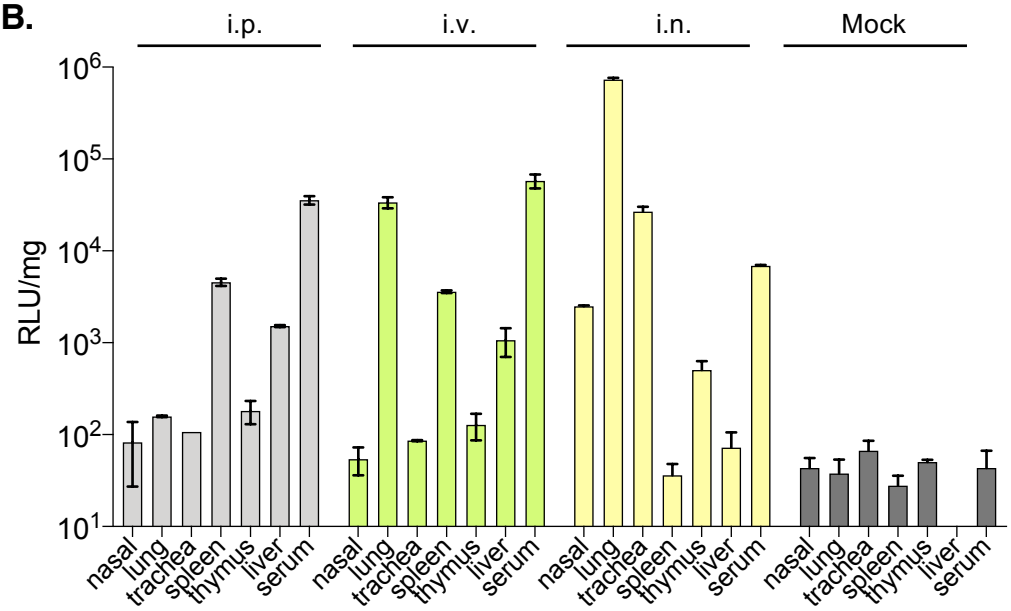

C.

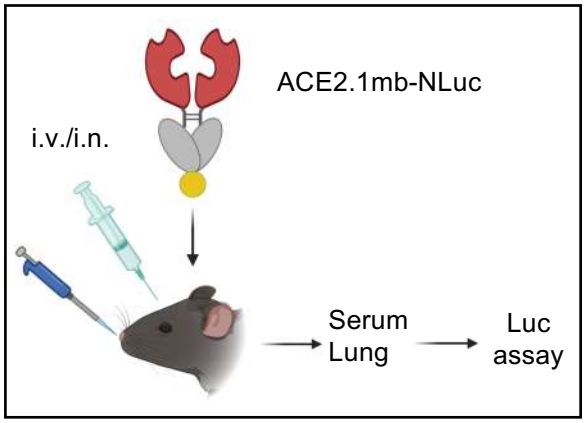

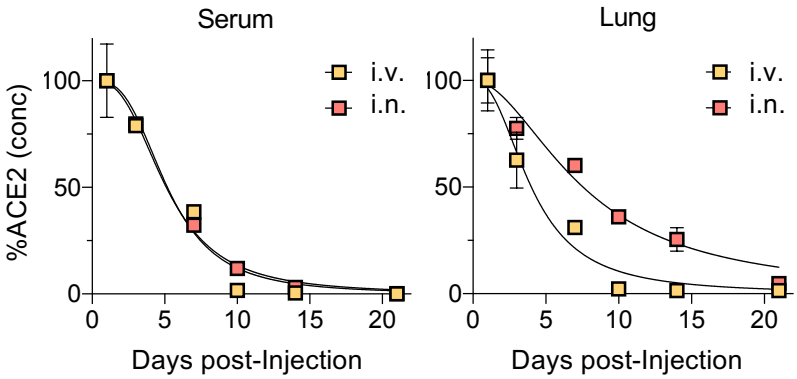

Serum		Lung	
i.v.	i.n.	i.v.	i.n.
5.2 days	5.1 days	4.0 days	7.6 days

Figure. 2

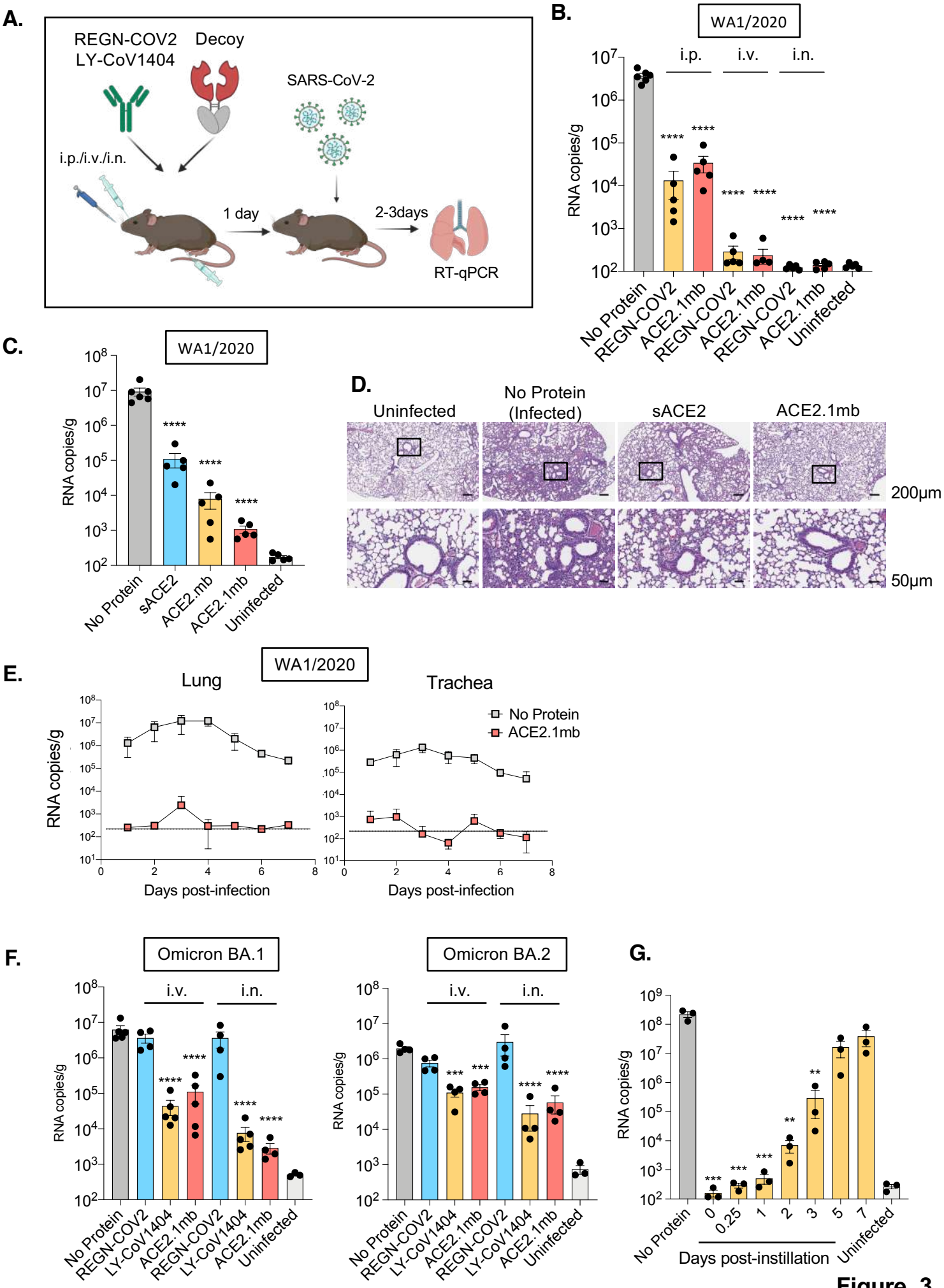
A.
REGN-COV2
LY-CoV1404
Decoy
SARS-CoV-2
i.p./i.v./i.n.
1 day
2-3days
RT-qPCR
B.
WA1/2020
i.p.
i.v.
i.n.
RNA copies/g
No Protein
REGN-COV2
ACE2.1mb
REGN-COV2
ACE2.1mb
REGN-COV2
ACE2.1mb
Uninfected
C.
WA1/2020
RNA copies/g
No Protein
sACE2
ACE2.mb
ACE2.1mb
Uninfected
D.
Uninfected
No Protein
(Infected)
sACE2
ACE2.1mb
200μm
50μm
E.
WA1/2020
Lung
Trachea
No Protein
ACE2.1mb
RNA copies/g
Days post-infection
Days post-infection
F.
Omicron BA.1
Omicron BA.2
i.v.
i.n.
RNA copies/g
No Protein
REGN-COV2
LY-CoV1404
ACE2.1mb
REGN-COV2
LY-CoV1404
ACE2.1mb
Uninfected
G.
RNA copies/g
No Protein
0
0.25
1
2
3
5
7
Uninfected
Days post-instillation

Figure. 3

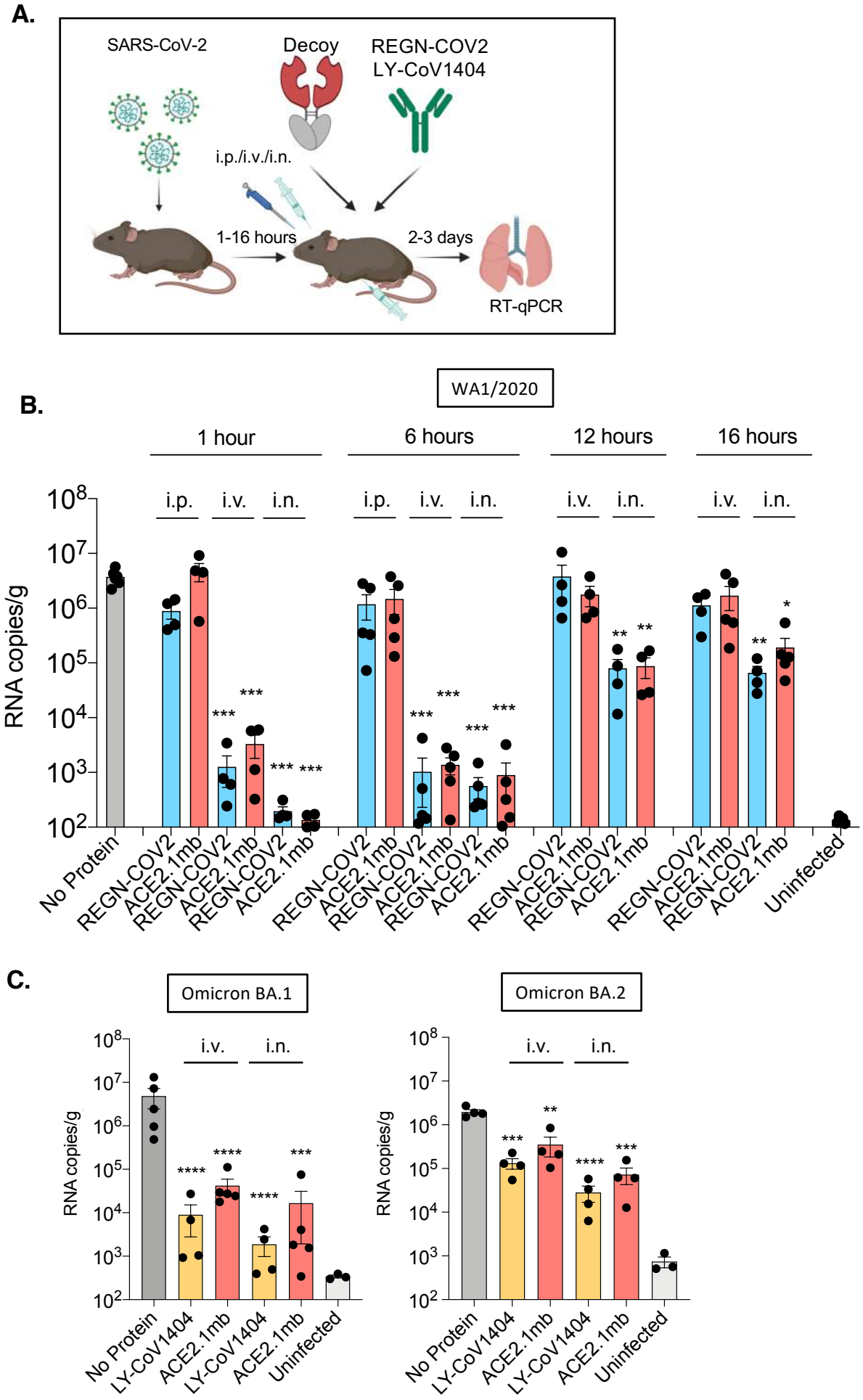
A.
SARS-CoV-2
Decoy
REGN-COV2
LY-CoV1404
i.p./i.v./i.n.
1-16 hours
2-3 days
RT-qPCR
B.
WA1/2020
1 hour
6 hours
12 hours
16 hours
i.p.
i.v.
i.n.
RNA copies/g
No Protein
REGN-COV2
ACE2.1mb
Uninfected
C.
Omicron BA.1
Omicron BA.2
LY-CoV1404

Figure. 4

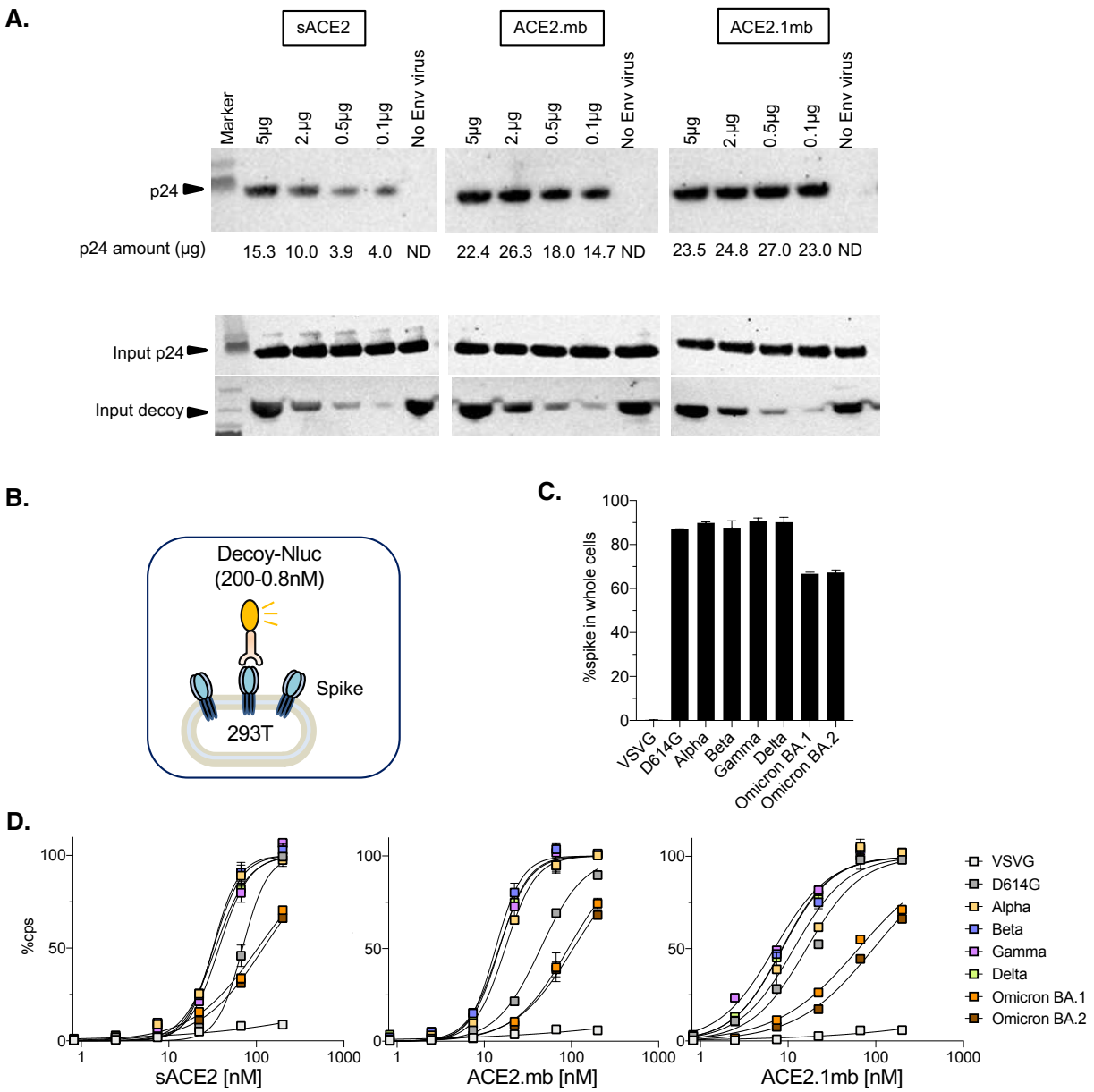

	50% binding (nM)							
	VSVG	D614G	Alpha	Beta	Gamma	Delta	Omicron BA.1	Omicron BA.2
sACE2	ND	69.48	32.25	31.87	37.35	34.18	104.1	120
ACE2.mb	ND	44.18	17.36	13.49	14.74	14.89	91.85	104.8
ACE2.1mb	ND	16.25	11.65	8.641	6.987	8.515	63.76	94.21

Supplementary Figure 1. Increased affinity of ACE2.1mb for the spike protein.

(A) Ni-NTA agarose beads were coated with different amounts (5, 2, 0.5, 0.1 µg) of sACE2, ACE2.mb or ACE2.1mb. A fixed amount of lentiviral virions pseudotyped with the D614G spike protein (30 µl) or control virions lacking the spike were incubated with the beads. After 1 hour,

free virions were removed by centrifugation and the remaining bead-bound virions were detected on an immunoblot probed with anti-p24 antibody. The amount of bead-bound p24 capsid protein was calculated against a standard curve with recombinant capsid and is indicated below each lane. Input virions and decoy proteins were detected on an immunoblot probed with anti-p24 and anti-His antibody and are shown below. ND: Not detected.

(B) The decoy:spike binding assay is diagrammed (left). 293T cells were transfected with 2 μg pcDNA-6 expression vectors for the VOC spike proteins. The cells were incubated at 37° with different amounts of decoy:luciferase fusion proteins. After 1 hour, unbound protein was removed by centrifugation and the amount of bound decoy protein was determined by luciferase assay. The amount of spike protein on the transfected 293T cells was analyzed by flow cytometry with anti-spike monoclonal antibody against the S2 protein (right). Avidity or the decoys is shown as curves with 100% binding set as luciferase activity at 400 nM decoy (below). The table shows the decoy concentration required for 50% maximal binding. The experiment was done three times with similar results.

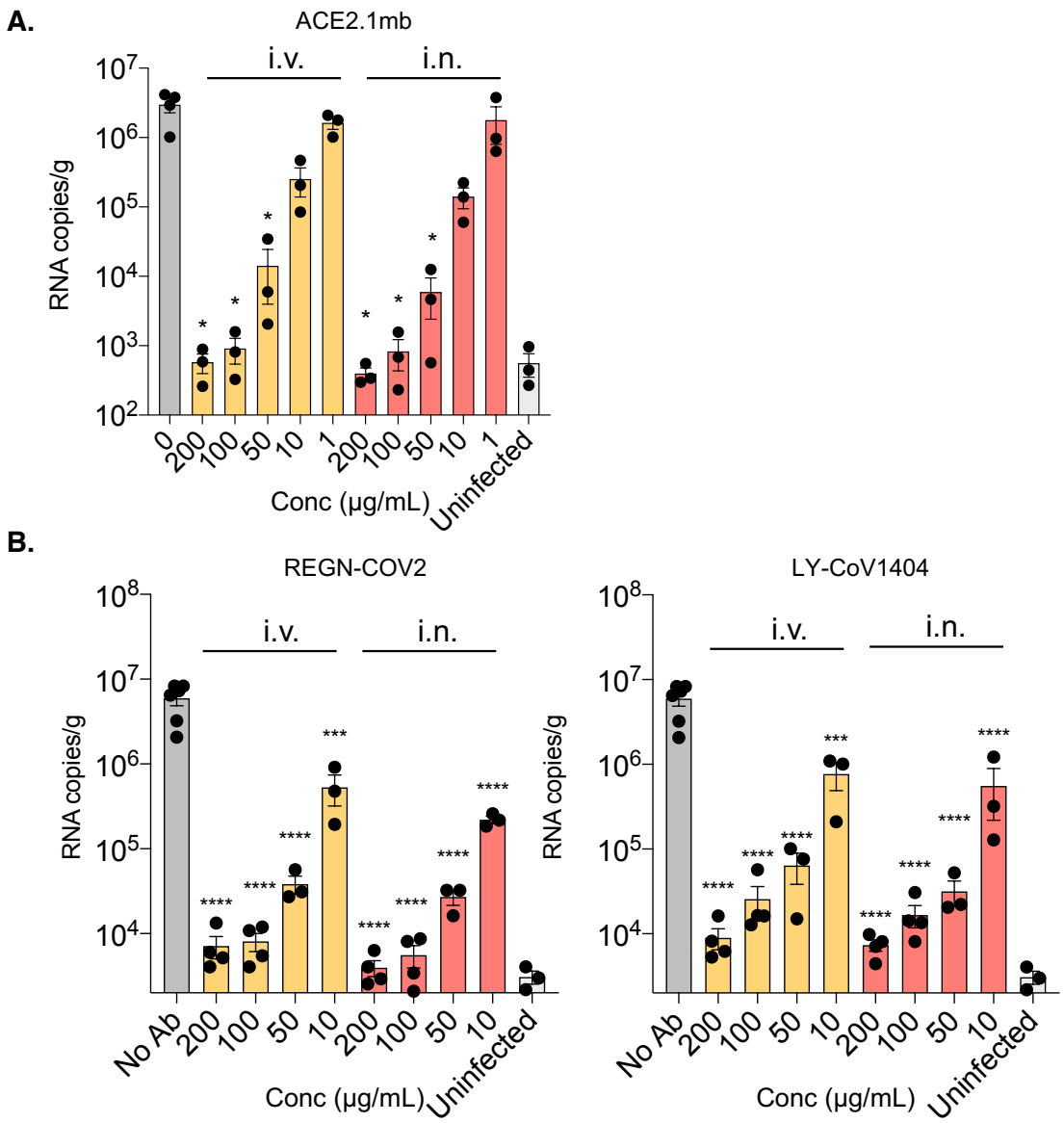

Supplementary Figure 2. Decoy and therapeutic monoclonal antibodies protect mice from SARS-CoV-2 infection.

(A) hACE2KI mice were injected i.v. or instilled i.n. with different amounts of decoy proteins. At 1-dpi, the mice were challenged with 2 X 10^4 PFU SARS-CoV-2 USA-WA1/2020 (n=3). 3-dpi, lung subgenomic viral E RNA was quantified by RT-qPCR.

(B) hACE2KI mice were injected i.v. or instilled i.n. with different amounts of REGN-COV2 or LY-CoV1404 antibody (n=3). At 1-dpi, the mice were challenged with 2 X 10^4 PFU of SARS-CoV-2 USA-WA1/2020. At 3-dpi, lung subgenomic viral E RNA was quantified by RT-qPCR.